Supplement of The Cryosphere, 17, 4297–4314, 2023
https://doi.org/10.5194/tc-17-4297-2023-supplement

The Cryosphere Open Access EGU

Supplement of

Mapping age and basal conditions of ice in the Dome Fuji region, Antarctica, by combining radar internal layer stratigraphy and flow modeling

Zhuo Wang et al.

Correspondence to: Olaf Eisen (olaf.eisen@awi.de)

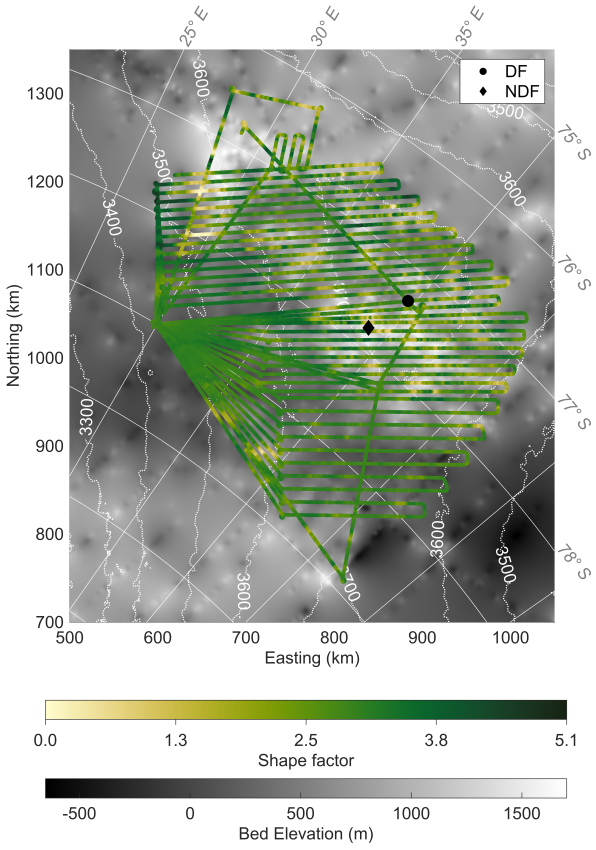

Figure S1. Shape factor along the profiles of the radar survey in the DF region. The interpolated shape factors at the DF drill site and the NDF are 3.1 and 2.2, respectively.

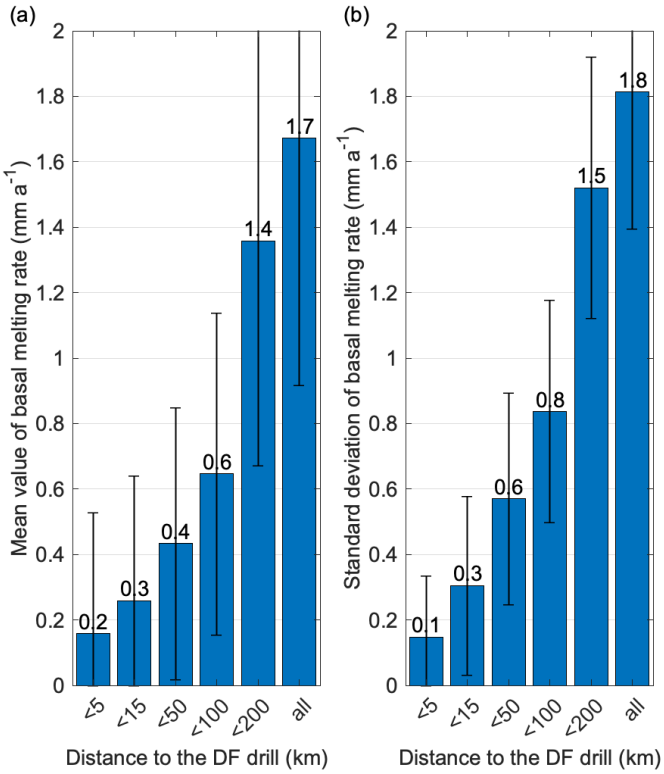

Figure S2. (a) Spatial mean value and (b) spatial standard deviation of deduced basal melt rates within 5, 15, 50, 200 km to the DF drill site. Error bars show the corresponding mean value and spatial standard deviation of uncertainties of basal melt rates, which are output together with melt rates from the model. The last bar "all" represents the whole study area. Numbers on the bars indicate the actual values.

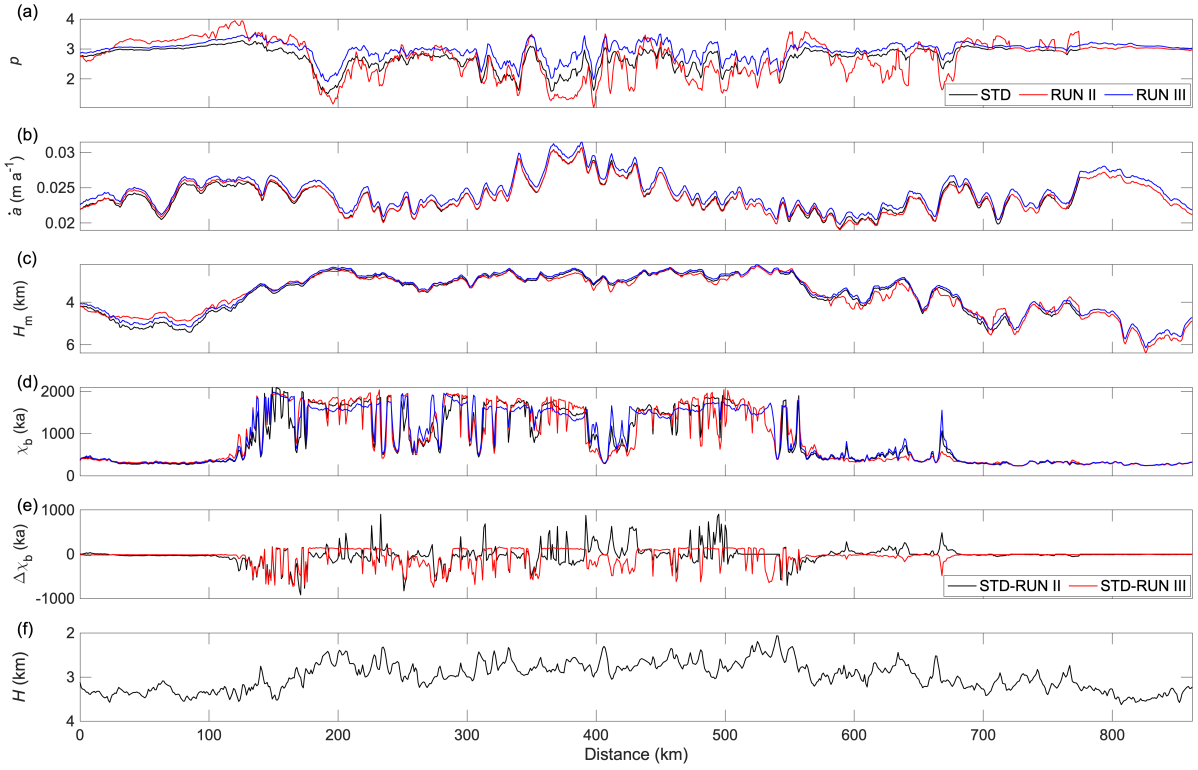

Figure S3. Comparison of (a) shape factor p, (b) accumulation rate $\dot{a}$, (c) mechanical ice thickness H_m, (d) age of basal ice χ_b for three runs (black line: STD, red line: RUN II, blue line: RUN III). (e) The difference of age of basal ice $\delta\chi_b$ between STD and RUN II (black), and between STD and RUN III (red). (f) Ice thickness H observed with radar (Karlsson et al., 2018). An overlap between STD and RUN II implies that there is no additional information of the EH8 in those areas (514–543 km, 644–650 km, 705–708 km, 722–744 km, 757–765 km and 776–863 km), which means the results of the two runs are similar and return same results. We find that difference of the shape factor (Fig. S3a) between STD and RUN II are relatively significant along the profile, especially at the distance from $\sim$ 0 km to $\sim$ 120 km, and from $\sim$ 590 km to $\sim$ 780 km (excluding the overlap areas). While STD and RUN III basically keep a similar difference in the whole profile, the shape factor of STD stays smaller than in RUN III. The difference of accumulation rates between STD and RUN III has a similar value of $\sim$ 0.0007 at each point along the profile, while the difference between STD and RUN II is negligible (Fig. S3b). The difference of mechanical ice thickness between STD and RUN II/RUN III are larger from 0 to 110 km, and from 580 to 710 km. In other places, the difference is tiny (Fig. S3c). From 580 to 700 km, we can observe a more spatially varying difference between STD and RUN II than RUN III. The age of basal ice at different points along the profile has a notable difference (Fig. S3d). For clarity we show the difference additionally between each two model runs in Fig. S3e. Occasional peaks of STD minus RUN III, e.g. at distance of $\sim$ 150 km, $\sim$ 170 km and $\sim$ 530 km, reach a difference of up to $\sim$ 800 ka. The differences between STD and RUN II is larger, up to $\sim$ 920 ka at $\sim$ 250 km, where EH8 was not traced the difference is 0. We find that the peaks in difference between STD and RUN II and III can be often observed at the same places, e.g. $\sim$ 150 km, $\sim$ 250 km, $\sim$ 490 km, together with peaks of bed topography (Fig. S3f), which implies that the topography is a important factor for age.

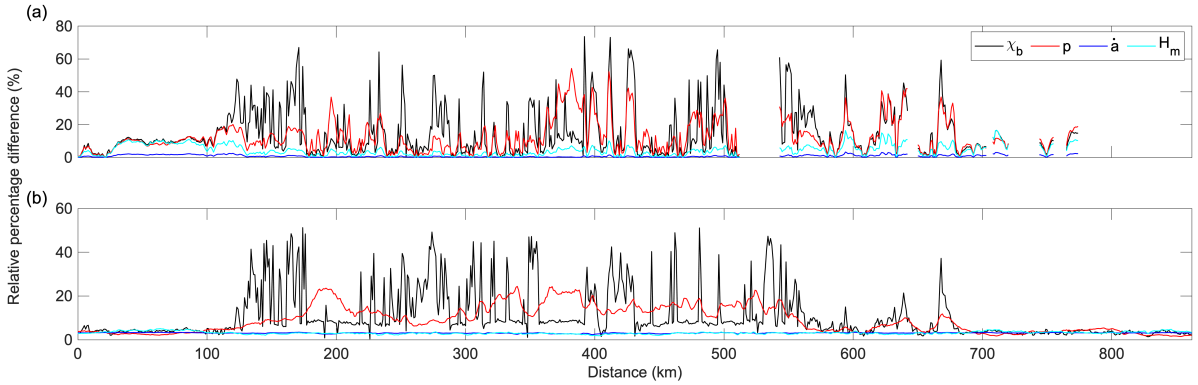

Figure S4. Relative percentage difference of the accumulation rate $\dot{a}$, the shape factor p, the mechanical ice thickness H_m and the age of basal ice χ_b derived from (a) STD minus RUN II, (b) STD minus RUN III. We find that at many points the relative percentage difference of the shape factor and the age of basal ice fluctuate simultaneously, e.g., from 0 to 100 km in Fig. S4a. However, such a synchronous behaviour does not always prevail, e.g. from 140 km to 150 km in Fig. S4a, and from 350 km to 400 km in Fig. S4b. The fluctuations of relative percentage difference of the accumulation rate in both scenarios are tiny along the profile. The relative percentage difference of mechanical ice thickness between STD minus RUN II basically follow the change of relative percentage difference of the shape factor, but with a much lower value.

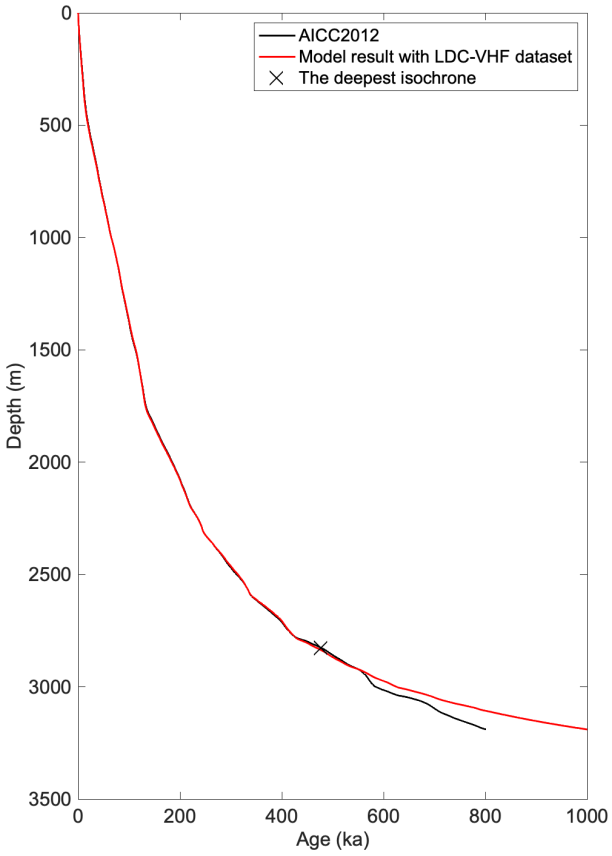

Figure S5. Model derived age–depth scale and AICC2012 timescale at EDC. (Chung et al., 2023)